

<sup>54</sup>Fe. However, no definite spin assignments have been made for high-spin states in this nucleus. This results from the disalignment of the 6528-keV level whose mean life was determined to be  $517 \pm 45$  ns. Shell-model calculations for high-spin states give results that are very different from those obtained for the proton particle-hole conjugate system <sup>50</sup>Ti and which do not follow the simple systematics found for <sup>50</sup>Ti and <sup>52</sup>Cr. In the excitation-energy region between 6 and 8 MeV in which there are states with spins greater than 8, the calculations reveal numerous states with spins between 8<sup>+</sup> and 11<sup>+</sup>. A value of +0.66 is computed for the *g* factor of the lowest-lying 10<sup>+</sup> state, which is to be compared to the experimental value of  $+0.78 \pm 0.02$  for the long-lived 6528-keV (10<sup>+</sup>) level.<sup>11</sup> Because of the scarcity of experimental data, the correspondence cannot be as easily established as for <sup>50</sup>Ti and <sup>52</sup>Cr. In these states not only proton excitations occur with a finite probability, but also neutron excitations to the  $1f_{5/2}$  and  $2p_{1/2}$  orbits become impor-

tant.

<sup>(a)</sup>Permanent address: Laboratoire de Physique Nucléaire, Université de Montréal, Québec, Canada.

<sup>1</sup>R. L. Auble, Nucl. Data Sheets 19, 291 (1976).

<sup>2</sup>A. Berinde *et al.*, Nucl. Phys. A284, 65 (1977), and references therein.

<sup>3</sup>B. A. Brown, D. B. Fossan, J. M. McDonald, and K. A. Snover, Phys. Rev. C 9, 1033 (1974), and references therein.

<sup>4</sup>I. P. Johnstone and H. G. Benson, J. Phys. G 3, L69 (1977).

<sup>5</sup>A. R. Poletti, B. A. Brown, D. B. Fossan, and E. K. Warburton, Phys. Rev. C 10, 2329 (1974).

<sup>6</sup>A. E. Litherland and A. J. Ferguson, Can. J. Phys. 39, 788 (1961).

<sup>7</sup>F. A. Beck, T. Byrski, A. Knipper, and J. P. Vivien, Phys. Rev. C 13, 1792 (1976).

<sup>8</sup>J. Styczen *et al.*, to be published.

<sup>9</sup>T. T. S. Kuo and G. E. Brown, Nucl. Phys. A114, 241 (1968).

<sup>10</sup>A. Müller-Arnke and R. D. Lawson, to be published.

<sup>11</sup>J. W. Noé, D. F. Geesaman, P. Gural, and G. D. Sprouse, Bull. Am. Phys. Soc. 22, 528 (1977).

## Elastic Scattering of 162-MeV Pions by Nuclei

B. Zeidman, C. Olmer, D. F. Geesaman, R. L. Boudrie, R. H. Siemssen,<sup>(a)</sup> J. F. Amann, C. L. Morris, H. A. Thiessen, G. R. Bureson, M. J. Devereux, R. E. Segel, and L. W. Swenson

Argonne National Laboratory, Argonne, Illinois 60439, and University of Colorado, Boulder, Colorado 80302, and Kernfysisch Versneller Instituut, Groningen, Netherlands, and Los Alamos Scientific Laboratory, Los Alamos, New Mexico 87544, and New Mexico State University, Las Cruces, New Mexico 88001, and Northwestern University, Evanston, Illinois 63301, and Oregon State University, Corvallis, Oregon 97331

(Received 21 February 1978)

The elastic scattering of 162-MeV  $\pi^+$  and  $\pi^-$  by <sup>9</sup>Be, Si, <sup>58</sup>Ni, and <sup>208</sup>Pb have been measured. All angular distributions, except for <sup>9</sup>Be, exhibit strong diffraction patterns. Optical-model calculations with matter distributions deduced from electron scattering qualitatively reproduce the data, but better agreement for all but <sup>9</sup>Be can be obtained with suitable modifications. No substantial differences in neutron- and proton-matter radii are indicated.

Elastic scattering of pions by complex nuclei provides information basic to the understanding of pion-induced nuclear reactions and the possibility of examining details of nuclear structure. At incident energies below 300 MeV, pion-nucleus interactions are dominated by the  $J = \frac{3}{2}$ ,  $T = \frac{3}{2}$  resonance in the pion-nucleon system, and a broad base of data in the resonance region is required. However, experimental investigations of the elastic and inelastic scattering of pions with high resolution at energies in the vicinity of the reso-

nance have only recently become feasible. In this Letter, we report data for the elastic scattering of both  $\pi^+$  and  $\pi^-$  by <sup>9</sup>Be, Si, <sup>58</sup>Ni, and <sup>208</sup>Pb at  $E_\pi = 162$  MeV, approximately the resonance energy in complex nuclei. These are the initial results of a survey of pion elastic scattering being performed at LAMPF (Clinton P. Anderson Meson Physics Facility) with the use of the EPICS spectrometer system.

A complete description of EPICS is presented elsewhere.<sup>1</sup> Briefly, the system consists of a

channel which provides a vertically dispersed beam on target and a spectrometer which is composed of magnetic dipoles, bending in the vertical plane, preceded by a magnetic quadrupole triplet. Multiwire counters located behind the triplet as well as behind the dipoles provide trajectory information so that the incident pion energy, emergent pion energy, and scattering angle are determined. The total momentum spread of the beam is  $\sim \pm 1\%$ , the point resolution is  $\Delta p/p \approx 2 \times 10^{-4}$ , and the angular resolution is less than  $1^\circ$ . During this experiment, the  $\pi^+$  flux was  $\sim 5 \times 10^7/\text{sec}$  and the  $\pi^-$  flux was about a factor of 5 lower.

The targets used in the present experiment were  $^9\text{Be}$  (105 mg/cm<sup>2</sup>),  $^{58}\text{Ni}$  (292 mg/cm<sup>2</sup>),  $^{208}\text{Pb}$  (289 mg/cm<sup>2</sup>), and natural Si (366 mg/cm<sup>2</sup>). The results of these calculations are displayed as the solid lines in Figs. 2(a) and 2(b), and the parameters used are listed in Table I. These calculations qualitatively reproduce the experimental results, but fail to predict accurately the observed minima locations. In fact, it is not possible to choose any reasonable set of neutron-density-distribution parameters that produces satisfactory agreement with both the  $\pi^+$  and  $\pi^-$  data, if the proton distribution is deduced from analyses of electron scattering.

Since the oscillation frequency in a strong-absorption model is determined by the product of a momentum and a radius, the observed discrepancy between the calculations and the experimental results suggests that the present optical-model prescription apparently overestimates at least one of these parameters. We therefore performed calculations with artificially reduced momenta or radii, as is also implied in other studies.<sup>10</sup> For

TABLE I. Matter distribution parameters for optical-model calculations. The values for the half-density radius,  $R$ , and diffuseness,  $a$ , are deduced from electron scattering (Ref. 9) with the relations  $\langle r^2 \rangle_{\text{electron}}^{1/2} = [\langle r^2 \rangle_{\text{charge}} - (0.8 \text{ fm})^2]^{1/2}$  and  $\frac{5}{3} \langle r^2 \rangle = R^2 + \frac{4}{3} \pi^2 a^2$ . The "modified" parameters are chosen so that  $\langle r^2 \rangle_{\text{modified}}^{1/2} = [\langle r^2 \rangle_{\text{charge}} - (1.3 \text{ fm})^2]^{1/2}$  and  $a$  is adjusted for optimum agreement with the data.

Nucleus	Charge	Electron		Modified			
	$\langle r^2 \rangle^{1/2}$ (fm)	$\langle r^2 \rangle^{1/2}$ (fm)	$R$ (fm)	$a$ (fm)	$\langle r^2 \rangle^{1/2}$ (fm)	$R$ (fm)	$a$ (fm)
$^9\text{Be}$	2.52	2.39	1.75	0.53	2.15	2.21	0.35
$^{28}\text{Si}$	3.10	2.99	2.82	0.55	2.80	2.47	0.55
$^{58}\text{Ni}$	3.76	3.67	3.97	0.54	3.52	3.68	0.55
$^{208}\text{Pb}$	5.50	5.44	6.51	0.55	5.34	6.26	0.60

example, reasonable agreement with the data is obtained for Si,  $^{58}\text{Ni}$ , and  $^{208}\text{Pb}$  when the rms radii were adjusted such that  $\langle r^2 \rangle_{\text{matter}} = \langle r^2 \rangle_{\text{charge}} - (1.3 \text{ fm})^2$ . The results of these calculations are shown as the dashed lines in Figs. 2(a) and 2(b); the parameters are listed in Table I. This procedure also produces agreement with the data for both  $\pi^+$  and  $\pi^-$  scattering from C at 162 MeV. Equally satisfactory agreement is achieved, however, if the density distributions retain the values derived from electron scattering, but the calculations are performed for incident pions whose energies range from 5 MeV (Pb) to 12 MeV (Si) lower than in the actual experiment. These latter calculations produce deeper minima for  $\pi^+$  scattering than are seen in calculations for the correct beam energy. The size of each of the targets exceeded the size of the beam spot on target (16 cm  $\times$  6 cm). Energy spectra for the spectra for the scattering of  $\pi^+$  from these targets are shown in Fig. 1. Similar spectra were obtained for the scattering of  $\pi^-$ . The measured energy resolution, approximately 350 keV, is limited by the target thickness, but it is clear that the energy resolution for all targets is more than adequate for completely resolving the ground-state from excited-state transitions. Radiative effects<sup>2</sup> which become apparent at the present level of resolution contribute to the small asymmetry in the peak shape with a low-energy tail.

Relative differential cross sections were obtained by normalization to the pion flux measured with an ionization chamber situated at  $0^\circ$ , downstream of the target. Absolute cross sections are based upon comparison with pion scattering from carbon at the same energy<sup>3</sup> in which the differential cross sections for carbon were determined relative to experimental values for the scattering of pions by hydrogen<sup>4</sup> at 162 MeV. These  $\pi$ -C elastic scattering cross sections are in excellent agreement with those recently measured by Piffaretti *et al.*<sup>5</sup> Corrections due to radiative effects are estimated to be only a few percent<sup>2</sup> and have not been included in the normalization. The uncertainty in absolute cross sections is estimated to be less than  $\pm 10\%$  and relative cross sections are accurate to better than  $\pm 5\%$ , ignoring purely statistical errors.

The angular distributions for the observed elastic scattering of 162-MeV  $\pi^+$  and  $\pi^-$  from  $^9\text{Be}$ , Si,  $^{58}\text{Ni}$ , and  $^{208}\text{Pb}$  are displayed in Figs. 2(a) and 2(b), respectively. (A tabulation of these cross sections is available on request.) Pronounced oscillations characteristic of strong pion absorption

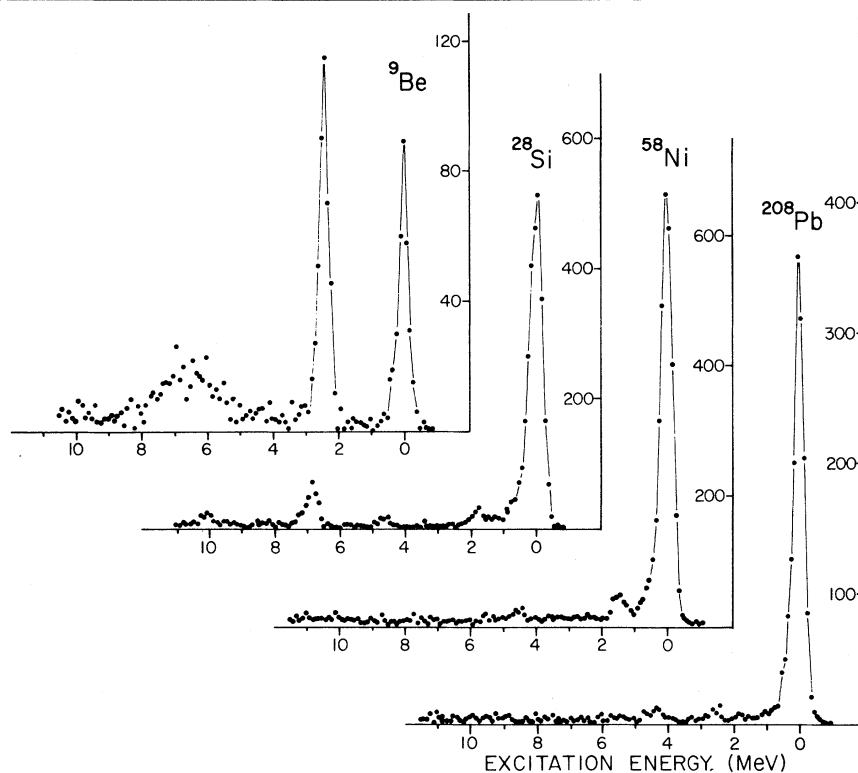


FIG. 1. Energy spectra obtained for the scattering of 162-MeV  $\pi^+$  by  $^9\text{Be}$ , Si,  $^{58}\text{Ni}$ , and  $^{208}\text{Pb}$  at a laboratory angle of  $50^\circ$ . Each datum point corresponds to approximately 100 keV.

are observed in the angular distributions for Si,  $^{58}\text{Ni}$ , and  $^{208}\text{Pb}$ . The data for scattering from  $^9\text{Be}$ , however, show relatively weak oscillatory structure.

A comparison of  $\pi^+$  and  $\pi^-$  elastic scattering from each of the targets is displayed in Fig. 2(c). For each target, comparable peak-to-valley ratios are observed for the oscillations in both  $\pi^+$  and  $\pi^-$  scattering. As is shown by calculations neglecting the Coulomb interaction, the shifts in oscillation frequency and locations in minima primarily result from Coulomb effects which introduce an overall phase difference between  $\pi^+$  and  $\pi^-$  scattering in addition to changing the local kinetic energy.

Optical-model calculations for the elastic scattering of 162-MeV  $\pi^+$  and  $\pi^-$  by  $^9\text{Be}$ ,  $^{28}\text{Si}$ ,  $^{58}\text{Ni}$ , and  $^{208}\text{Pb}$  have been performed using the momentum-space elastic-scattering code PIPIT.<sup>6</sup> The collision matrix is calculated using free-pion-nucleon phase shifts<sup>7</sup> and a model<sup>8</sup> for offshell extrapolation. The effects of nucleon Fermi motion have been neglected. The nuclear-matter distributions were assumed to be of Woods-Saxon form, with identical parameters specifying pro-

ton and neutron distributions.

Initially, the matter distributions were obtained from the charge distributions determined by analyses of electron scattering<sup>9</sup> with a correction for the finite charge radius of the proton. This results from changes in both the pion-nucleon and Coulomb interaction which are evaluated at the new energy. It is also noteworthy that both the modified and unmodified calculations predict virtually identical cross sections at forward angles, all agreeing with the measured values for Si,  $^{58}\text{Ni}$ , and  $^{208}\text{Pb}$ . The gross disagreements between data and calculations for  $^9\text{Be}$  are indicative of the fact that the current procedure is inappropriate, and may be due to the nonzero spin or unusual structure of the weakly bound  $^9\text{Be}$  system.

Further calculations were performed with the "modified" proton-distribution parameters listed in the table and the neutron distributions varied. It was found that for  $^{208}\text{Pb}$  the agreement with the data becomes significantly worse if the difference between neutron and proton radii is as much as 0.2 fm. A similar sensitivity to the neutron radius is deduced for  $^{28}\text{Si}$ . These results are consistent with earlier studies<sup>11</sup> of nuclear mat-

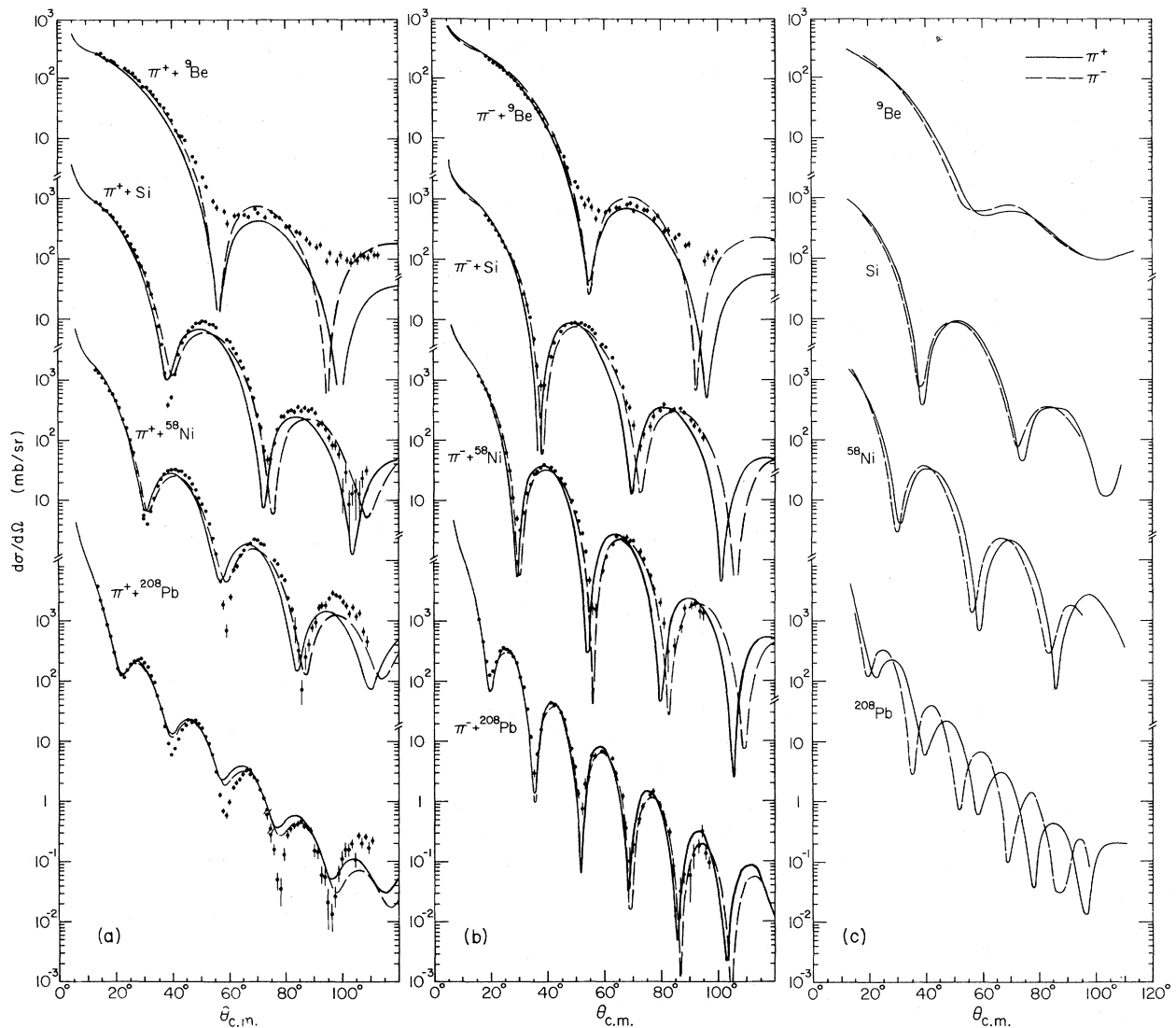


FIG. 2. Angular distributions for the elastic scattering of 162-MeV (a)  $\pi^+$  and (b)  $\pi^-$  by  ${}^9\text{Be}$ , Si,  ${}^{58}\text{Ni}$ , and  ${}^{208}\text{Pb}$ . The curves result from optical-potential calculations discussed in the text, and are displayed with no adjustment of magnitude. (c) Comparison of 162-MeV  $\pi^+$  and  $\pi^-$  elastic scattering from  ${}^9\text{Be}$ , Si,  ${}^{58}\text{Ni}$ , and  ${}^{208}\text{Pb}$ . The lines are smooth curves drawn through the data points of (a) and (b).

ter distributions which indicate little, if any, difference in the proton and neutron radii of these nuclei.

In conclusion, angular distributions were measured for the elastic scattering of 162-MeV  $\pi^+$  and  $\pi^-$  by  ${}^9\text{Be}$ , Si,  ${}^{58}\text{Ni}$ , and  ${}^{208}\text{Pb}$ . Optical-model calculations indicate that qualitative differences between  $\pi^+$  and  $\pi^-$  elastic scattering are primarily due to the Coulomb interaction, and that possible differences in the proton- and neutron-matter radii appear to be small ( $\sim 0.1$  fm). These calculations reproduce the data better if the matter radii deduced from electron scattering or the in-

cident energy in the calculations are decreased. The necessity for these adjustments indicates the need for improved models and a greater understanding of pion-nucleus interactions.

We wish to acknowledge the aid and assistance provided by the LAMPF staff and those who have contributed to the development of EPICS. We appreciate several helpful discussions with Dr. T.-S. H. Lee, Dr. B. Gibson, Dr. W. Gibbs, Dr. G. E. Stephenson, and Dr. E. T. Boschitz.

Work performed under the auspices of the U. S. Department of Energy and the National Science Foundation.

<sup>(a)</sup>Work performed while a visitor at Argonne National Laboratory, Argonne, Ill. 60439.

<sup>1</sup>H. A. Thiessen *et al.*, to be published, and LASL Report No. LA-4534 MS, 1970 (unpublished).

<sup>2</sup>E. Borie, *Phys. Lett.* **68B**, 433 (1977).

<sup>3</sup>K. Boyer *et al.* to be published.

<sup>4</sup>P. J. Bussey, J. R. Carter, D. R. Dance, D. V. Bugg, A. A. Carter, and A. M. Smith, *Nucl. Phys.* **B58**, 363 (1973).

<sup>5</sup>J. Piffaretti, R. Corfu, J. P. Egger, P. Gretillat, C. Lunke, E. Schwarz, C. Perrin, and B. M. Preedom, *Phys. Lett.* **71B**, 324 (1977).

<sup>6</sup>R. A. Eisenstein and F. Tabakin, *Comput. Phys. Commun.* **12**, 237 (1976).

<sup>7</sup>D. H. Herndon, A. Barbaro-Galtieri, and A. H. Ro-

senfeld, Lawrence Radiation Laboratory Report No. UCRL-20030  $\pi N$ , 1970 (unpublished).

<sup>8</sup>J. Londergan, R. McVoy, and E. Moniz, *Ann. Phys.* (N.Y.) **86**, 147 (1974).

<sup>9</sup>C. W. DeJager, H. DeVries, and C. DeVries, *At. Data Nucl. Data Tables* **14**, 479 (1974).

<sup>10</sup>E. T. Boschitz, in *Proceedings of the International Conference on High-Energy Physics and Nuclear Structure, Zurich, 1977*, edited by M. P. Locher (Birkhauser-Verlag, Basel, Switzerland), p. 133, and private communication.

<sup>11</sup>E.g., J. A. Nolen and J. P. Schiffer, *Annu. Rev. Nucl. Sci.* **10**, 471 (1969); S. Shlomo and E. Friedman, *Phys. Rev. Lett.* **39**, 1180 (1977), and references therein.

## Precision Laser Photodetachment Spectroscopy in Magnetic Fields

W. A. M. Blumberg, R. M. Jopson, and D. J. Larson

*Lyman Laboratory of Physics, Harvard University, Cambridge, Massachusetts 02138*

(Received 15 March 1978)

Magnetic-field-dependent structure in the photodetachment cross section of negative sulfur ions has been observed. This is the first observation of such structure for any negative ion. The structure is found to be due in part to the excitation of the detached electrons to discrete cyclotron levels.

We have observed the effect of a strong magnetic field on the photodetachment cross section of the negative sulfur ion near the threshold for detachment from the  $^2P_{3/2}$  state. Part of the motivation for this investigation is the possibility that state-dependent photodetachment might provide an effective method of producing and detecting population differences in certain stored ionic species.  $S^-$  was selected for study because at zero magnetic field the photodetachment cross section near threshold is known to be a steeply rising monotonic function of light frequency.<sup>1</sup> We observed that the application of a magnetic field produces structure in the cross section which has a periodic dependence on the light frequency. This structure constitutes a dramatic departure from the behavior at zero magnetic field.<sup>1,2</sup> We find that the oscillatory structure is due to the excitation of the detached electron to discrete cyclotron (Landau) levels in the magnetic field.<sup>3</sup>

The only bound states of the group-VI series of atomic negative ions are  $^2P$  fine-structure doublet formed from a  $p^5$  configuration. The energy level diagram for  $S^-$  as measured by Lineberger and Woodward<sup>1</sup> is shown in Fig. 1. The dependence of the zero-field photodetachment cross section on photon energy was more clearly demonstrated

in experiments on  $Se^-$ . Hotop, Patterson, and Lineberger<sup>2</sup> found that  $\sigma \propto (\nu - \nu_{\text{threshold}})^{1/2}$ , thus verifying the Wigner prediction<sup>4</sup> for experimental resolution on the order of  $2 \text{ cm}^{-1}$  and for energies of less than  $40 \text{ cm}^{-1}$  above threshold. The measurements reported in this paper involve at

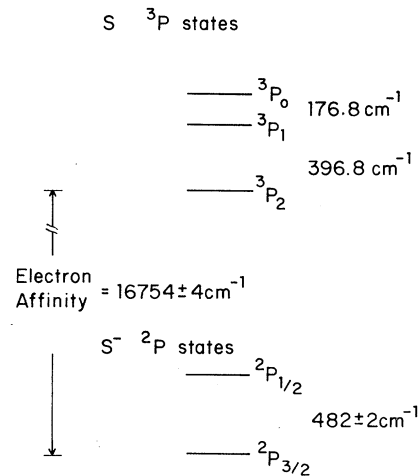


FIG. 1. Zero-field energy levels of  $S^-$  and S. The  $^2P_{3/2} \rightarrow ^3P_2$  transition has been used for all of the results reported in this paper.